

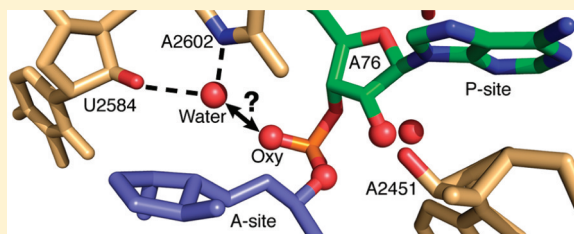
# Minimal Transition State Charge Stabilization of the Oxyanion during Peptide Bond Formation by the Ribosome

Nicolas Carrasco,<sup>†</sup> David A. Hiller, and Scott A. Strobel\*

Departments of Molecular Biophysics & Biochemistry and Chemistry, Yale University, 260 Whitney Ave., New Haven, Connecticut 06520-81114, United States

**S** Supporting Information

**ABSTRACT:** Peptide bond formation during ribosomal protein synthesis involves an aminolysis reaction between the aminoacyl  $\alpha$ -amino group and the carbonyl ester of the growing peptide via a transition state with a developing negative charge, the oxyanion. Structural and molecular dynamic studies have suggested that the ribosome may stabilize the oxyanion in the transition state of peptide bond formation via a highly ordered water molecule. To biochemically investigate this mechanistic hypothesis, we estimated the energetic contribution to catalytic charge stabilization of the oxyanion using a series of transition state mimics that contain different charge distributions and hydrogen bond potential on the functional group mimicking the oxyanion. Inhibitors containing an oxyanion mimic that carried a neutral charge and a mimic that preserved the negative charge but could not form hydrogen bonds had less than a 3-fold effect on inhibitor binding affinity. These observations argue that the ribosome provides minimal transition state charge stabilization to the oxyanion during peptide bond formation via the water molecule. This is in contrast to the substantial level of oxyanion stabilization provided by serine proteases. This suggests that the oxyanion may be neutralized via a proton shuttle, resulting in an uncharged transition state.



The ribosome catalyzes peptide bond formation during protein synthesis. This is a biologically essential reaction that occurs within the peptidyl transferase center (PTC) of the ribosomal 50S subunit at a rate approximately  $10^7$ -fold faster than the uncatalyzed reaction [recently reviewed in ref 1]. The reaction occurs when the  $\alpha$ -amino group of the aminoacyl tRNA in the A site nucleophilically attacks the carbonyl ester of the peptidyl tRNA in the P site (Figure 1A). As the nitrogen–carbon bond forms, the carbonyl carbon acquires tetrahedral geometry and the carbonyl oxygen develops a negative charge, resulting in an intermediate with a local energy minimum along the reaction coordinate. Subsequently, as the ester bond breaks and the double bond to the carbonyl oxygen re-forms, this intermediate collapses to produce a peptidyl tRNA elongated by one amino acid in the A site and a deacylated tRNA in the P site. Transition state characterization can help define how the ribosome promotes catalysis of this reaction relative to similar aminolysis reactions in solution.

Recent studies have provided substantial information about the chemical basis of peptide bond formation. High-resolution structures of the 50S subunit bound to the transition state inhibitor, CCdApPmn, demonstrated that the active site is made of RNA, which suggested that the ribosome is a ribozyme.<sup>2</sup> Specific functional groups important for the reaction have been identified including the 2'-OH group of the A76 peptidyl tRNA,<sup>3–5</sup> the 2'-OH group of A2451,<sup>6–8</sup> and two highly ordered water molecules.<sup>7,9</sup> The vicinal 2'-OH group of the tRNA has been proposed to contribute to catalysis by mediating a proton shuttle between the aminoacyl-tRNA  $\alpha$ -amino nucleophile and the peptidyl-tRNA O3' leaving

group.<sup>9,10</sup> Similarly, the A2451 2'-OH group within the 50S RNA has also been demonstrated to contribute to catalysis in biochemical studies, possibly by orienting the nucleophile.<sup>6–8</sup>

Other important features of the peptidyl transferase (PT) reaction have been identified using a series of novel transition state inhibitors. Structural studies of a chiral inhibitor that contained a sulfur and a methyl carboxylate at the nonbridging oxygen positions as mimics of the oxyanion and nascent peptide, respectively, suggested that the reaction proceeds via a transition state with tetrahedral-like geometry with *S* chirality.<sup>9,5</sup> Such a geometry means that the  $\alpha$ -amino group attacks the planar carbonyl carbon from the same face of the molecule as the peptidyl tRNA 2'-OH of A76. The establishment of the chirality of the reaction also defined the spatial position of the oxyanion in the transition state. Further evidence that the carbonyl carbon adopts tetrahedral-like geometry in the transition state comes from recent kinetic isotope effect (KIE) studies, which established that the rate-limiting step for the reaction involves N–C bond formation accompanied by significant deprotonation of the nucleophile.<sup>11</sup> A proton inventory measured by solvent isotope effects established that multiple protons are in flight during the transition state.<sup>12</sup>

A potential strategy the ribosome may use to promote peptide bond formation is stabilization of the developing oxyanion in the transition state. This would be analogous to

**Received:** August 12, 2011

**Revised:** October 5, 2011

**Published:** October 28, 2011



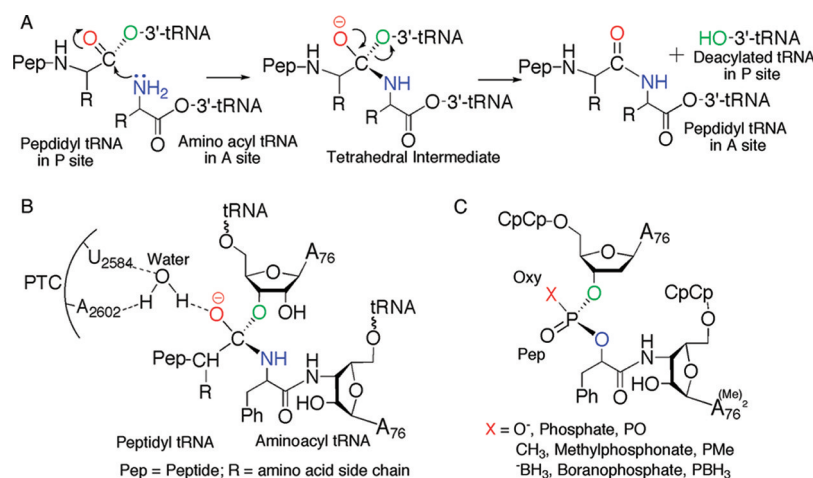


**Figure 1.** (A) The peptidyl transferase reaction. In the tetrahedral intermediate the  $\alpha$ -amine is drawn in the deprotonated form based on recent biochemical results.<sup>47</sup> (B) Possible model for the stabilization of the oxyanion in the transition state. (C) Generic structures of the hexameric peptidyl transferase oxyanion mimics.

mechanisms employed by serine proteases to promote peptide hydrolysis. High-resolution structural studies of the 50S ribosome in complex with a transition state mimic of the oxyanion identified a highly ordered water molecule that makes hydrogen-bonding contacts with the oxyanion in the active site.<sup>9</sup> This water molecule is coordinated via hydrogen bonds to two highly conserved residues within the ribosome, A2602 and U2584 (Figures 1B and 2). On the basis of the location of this

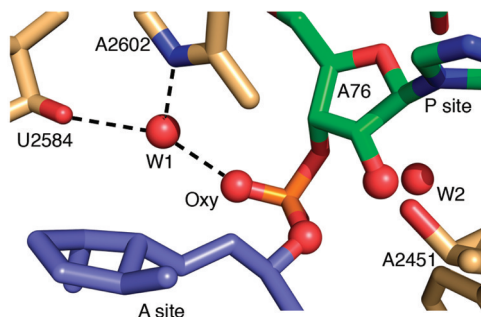


**Figure 2.** Functional groups within the peptidyl transferase center. 50S ribosome (golden) bound to the transition state inhibitor, CCA-p-hPmnCC. W1 represents the proposed water molecule that stabilizes the oxyanion; W2 represents another water molecule that might play a role in the proton shuttle mechanism; Oxy represents the oxyanion. Protein Data Bank entry 1VQP.<sup>9</sup>

water relative to the oxyanion, it was proposed that the water stabilizes the oxyanion in the transition state. This hypothesis was further supported by molecular dynamic simulation studies, which concluded that the polarizing effect of the water molecule is catalytically favorable both enthalpically and entropically.<sup>13</sup> But the role of this water molecule and its contribution to oxyanion stabilization have not been tested biochemically.

To explore this question, we investigated the magnitude of the interaction between the ribosome and the oxyanion. We prepared a series of peptidyl transferase transition state mimics that contain different charge distributions and hydrogen-bonding potentials at the oxyanion position and measured their relative affinity for the ribosome (Figure 1C). Here we present evidence indicating the peptidyl transferase center

provides minimal transition state stabilization to the oxyanion, which has implications for the nature of the catalysis provided by the ribosome during protein synthesis.

## MATERIALS AND METHODS

**Materials.** All solvents and reagents for solution and solid phase synthesis were purchased from Aldrich unless otherwise stated. NMR spectra were measured on Bruker Advance DPX-400 and Bruker Advance DPX-500 spectrometers. Mass spectra were collected on Waters Micromass LCT and Waters Micromass ZQ mass spectrometers. HPLC purification of inhibitors was carried out on a C18 reversed-phase Zorbax column (Hewlett-Packard). T4 polynucleotide kinase and PNK buffer were from New England Biolabs. Reverse transcriptase AMV and protector RNase inhibitor were from Roche. Nuclease P1 and snake venom phosphodiesterase were purchased from Worthington.

**Inhibitor Synthesis.** The inhibitors were prepared as hexanucleotides (CCdA-p(X)-hPmnCC) with a CCdA on the P-site side and hydroxyphurmycin-CC (hPmnCC) on the A-site side (Figure 1C). These two elements were joined via a phosphate or phosphate derivative linkage between the  $\alpha$ -hydroxyl of hPmn and the O3' of dA. This phosphate and its derivatives (where X is O, CH<sub>3</sub>, and BH<sub>3</sub>) serve as the mimic of the reaction's tetrahedral-like transition state. Shorter dinucleotide versions (dA-p(X)-hPmn) were prepared to assist with the stereochemical assignment of the full-length inhibitors. The inhibitors were synthesized using standard procedures in phosphoramidite solid-phase chemistry<sup>5,14</sup> following the synthetic scheme shown in Supporting Information Figure S3.

**Methylphosphonate Inhibitors [CCdA-p(CH<sub>3</sub>)-hPmnCC].** The synthesis of the methylphosphonate diastereomers involved coupling 5'-DMTr-N-benzoyl-2'-deoxy-adenosine,3'-[(methyl)-(N,N-diisopropyl)]phosphoramidite (Glen Research, Cat. #10-1100) with a suitably protected hydroxyphurmycin derivative, which was tethered to polystyrene beads via a succinate linkage (Supporting Information Figure S3). Synthesis of the immobilized hydroxyphurmycin derivative was carried out as described previously.<sup>5</sup> After oxidation of the phosphate backbone, capping, and removal of the DMTr groups, two coupling cycles were performed to incorporate the cytidine nucleotides simultaneously at both ends. Because of

the lability of the methylphosphonate linkage relative to the phosphate counterpart, we used the recommendations outlined by the Glen Research for cleavage, deprotection, and desalting. The two diastereomers were separated with baseline resolution by RP-HPLC on a Zorbax semiprep column (Hewlett-Packard) using a 50 mM triethylammonium acetate (TEAAc, pH 6.6)/acetonitrile gradient. Each of the purified diastereomers was analyzed by electrospray mass spectrometry. Because both methylphosphonate diastereomers bound to the ribosome with similar affinity, it was not necessary to establish the absolute stereochemistry.

#### Boranophosphate Inhibitor [CCdA-p(BH<sub>3</sub>)-hPmnCC].

The boranophosphate diastereomer was synthesized using DoD/ACE chemistry with minor modification (Supporting Information Figure S3). This chemical strategy was necessary because the borano group is incompatible with the trityl and acyl protecting groups.<sup>15</sup> The exocyclic amines of adenosine and cytidine were protected with the allyloxycarbonyl group as described.<sup>16</sup> Oxidation of the phosphate backbone to introduce the borano group was performed using 25 mM BH<sub>3</sub>·THF in THF for 10 min.<sup>17</sup> After synthesis, the allyloxycarbonyl groups were removed using palladium.<sup>18</sup> Cleavage from the polystyrene solid support was performed using 1:1 (v/v) ammonium hydroxide:methylamine (40% aqueous) using the fast deprotection procedure recommended by Glen Research. Purification and characterization were performed as described above.

**Defining the Stereochemistry of dA-p(BH<sub>3</sub>)-hPmn I and II.** The stereochemically pure dA-p(BH<sub>3</sub>)-hPmn I, dA-p(BH<sub>3</sub>)-hPmn II, and the control phosphate, dA-p-hPmn, were labeled at the 5'-end with <sup>32</sup>P using T4 polynucleotide kinase (PNK). The reaction mixtures were purified using polyacrylamide gel electrophoresis, and the bands corresponding to the desired products were excised and eluted in 200 μL of water. Each labeled inhibitor (5 μL) was incubated with 3 units of nuclease P1 (10 mM sodium acetate, pH 5.5, 0.5 mM ZnCl<sub>2</sub>) at 25 °C in a 50 μL reaction. Aliquots were removed and quenched with loading buffer at various times. The products of the reactions were resolved by 23% denaturing PAGE, and the results were analyzed.

**Partial Digestion of CCdA-p(BH<sub>3</sub>)-hPmnCC to dA-p(BH<sub>3</sub>)-hPmn.** Nonlabeled CCdA-p(BH<sub>3</sub>)-hPmnCC (3 nmol) was treated with 3 units of nuclease P1 as described above for 15 min. Antarctic phosphatase (20 units) was added to remove the 5'-phosphates at both ends. After 15 min, the reaction was diluted with 50 mM TEAAc (pH 6.6, 100 μL) and analyzed on RP-HPLC.

**Measurement of Inhibitor Binding Affinities.** The binding affinities of each inhibitor were measured by the efficiency of protection from chemical modification with dimethyl sulfate (DMS) at nucleotide A2602 as visualized by primer extension using previously described procedures.<sup>19</sup> The measured *K<sub>d</sub>* was used to calculate the relative change in free energy using the relationship  $\Delta G = -RT \ln(K_{d1}/K_{d2})$ , where *R* is the gas constant, *T* is temperature, *K<sub>d1</sub>* is the binding affinity of the reference phosphate inhibitor, and *K<sub>d2</sub>* is the binding affinity of the methylphosphonate or boranophosphate inhibitors.

## RESULTS

**Inhibitor Design.** To biochemically address how the ribosome stabilizes the developing negative charge in the transition state of peptide bond formation, we synthesized a

series of tetrahedral transition state mimics and measured their relative binding affinities for the ribosome (Figure 1C). These inhibitors are an expanded set based on the original inhibitor, CCdA-p-Pmn, reported by Welch et al.<sup>20</sup> They share the general structure 5'-CCdA-p(X)-hPmnCC-3', where 5'-CCdA and hPmnCC-3' represent the evolutionarily conserved 5'-CCA-3' ends of the P-site tRNA and A-site tRNA fragments, respectively (Figure 1C). These tRNA fragments are linked together via a modified 3'-3' phosphodiester linkage. The phosphorus, represented as a "p" in the general structure, mimics the tetrahedral carbon center in the reaction (Figure 2). Attached to the nonbridging positions of this phosphorus are the oxyanion mimic (X) and a second oxygen representing the nascent peptide. The inhibitors all have the same tetrahedral geometry. They differ in the charge distributions and hydrogen-bonding potentials of the functional groups that mimic the oxyanion. Structural studies have shown that inhibitors of the general structure CCdA-p-hPmnCC bind in the induced conformation to the PTC and that the presence of the 2'-deoxy substitution in the tRNA peptidyl position does not affect binding compared with the ribose counterpart.<sup>21</sup>

All four of the inhibitors are hexamers and include members with an oxygen (PO), a methyl group (PMe), or a borano group (PBH<sub>3</sub>) at the oxyanion position (Figure 1C). Two diastereomers for the methyl-containing hexamers were obtained, but only a single diastereomer was isolated for the PBH<sub>3</sub> inhibitor. One of the two PBH<sub>3</sub> diastereomers was chemically unstable, possibly due to the presence of the 3'-3' boranophosphodiester linkage (see Supporting Information).

For the purposes of this study, the PO inhibitor serves as a benchmark for comparison. The two nonbridging oxygen atoms of this inhibitor are equivalent (Figure 1C). The PMe inhibitor is chiral, neutral, and cannot efficiently form hydrogen bonds with the water molecule. Because of these properties, oligonucleotides containing such methylphosphonate linkages have been used to probe electrostatic and hydrogen bond interactions in DNA and RNA nucleases.<sup>22,23</sup> The PBH<sub>3</sub> inhibitor has a borano group in place of one of the nonbridging oxygen atoms and is also chiral [reviewed in ref 15]. It carries a formal negative charge like the PO inhibitor, but it cannot form hydrogen-bonding interactions.<sup>24</sup> Each of these inhibitors is expected to bind in a similar manner within the PTC. Their primary difference is the charge distribution and hydrogen-bonding potential at the oxyanion position.

Given that it is impossible to "mutate" a water molecule, this series of inhibitors offers an experimental approach to address the role of water within the PTC. It is expected that the inhibitor whose charge and hydrogen-bonding potential best complements the ribosomal PTC will bind with the highest affinity.<sup>25</sup> This type of analysis provides a measurable estimate of the energy of oxyanion stabilization provided by the ribosome. Although the methylphosphonate and boranophosphate substitutions could alter the energy of the free inhibitor, complicating our analysis, this effect is likely to be small. Numerous studies of methylphosphonate binding enzymes have shown no systematic effects on affinity, and positions that are not directly contacted by the enzyme often show no effect on binding.<sup>23,26</sup> Therefore, the difference in affinities of these compounds provides a reasonable estimate of energetic differences in the ribosome-inhibitor complexes.

**Assigning the Absolute Stereochemistry of the PBH<sub>3</sub> Inhibitors.** A significant challenge in this study was establishing the absolute stereochemistry of the inhibitors, most notably



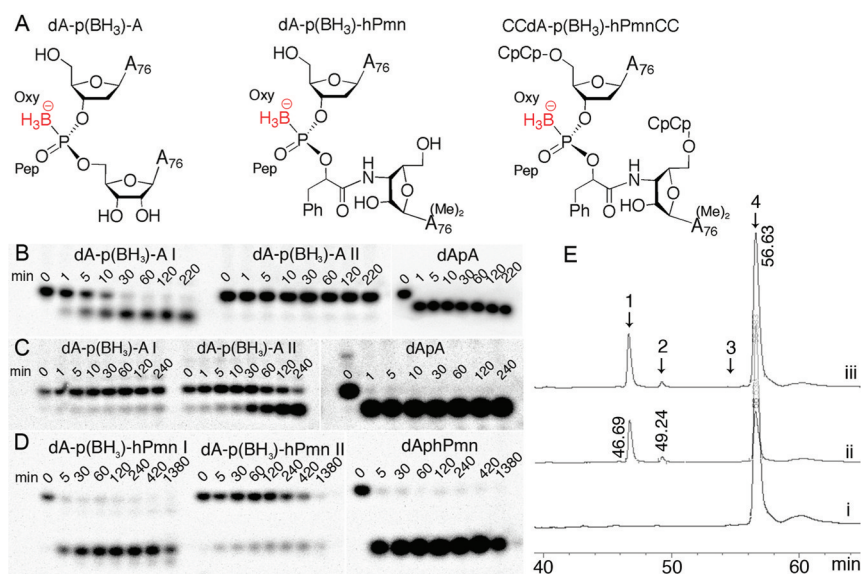


**Figure 3.** Determination of the absolute stereochemistry of the CCdA-p(BH<sub>3</sub>)-hPmnCC boranophosphate inhibitor. (A) Structural relationship of three boranophosphate molecules used in the assignment. Gel electrophoresis showing the digestion patterns of dA-p(BH<sub>3</sub>)-A I and II and dApA using SVP (B) or nuclease P1 (C); dApA is the reference dinucleotide that has a phosphate linkage. (D) Digestion patterns of dA-p(BH<sub>3</sub>)-hPmn I and II and dAphPmn using nuclease P1. (E) RP-HPLC analysis of the partial digestion of CCdA-p(BH<sub>3</sub>)-hPmnCC using nuclease P1 (only a section of the chromatogram is shown); the partial digestion product coeluted with the dinucleotide inhibitor dA-p(BH<sub>3</sub>)-hPmn II, peak at 56.63 min, shown by arrow 4 (independent experiments showed that dA-p(BH<sub>3</sub>)-hPmn I eluted at 54.59 min, shown by arrow 3; also see Figure S4): (i) pure dA-p(BH<sub>3</sub>)-hPmn II alone; (ii) product of partial digestion of CCdA-p(BH<sub>3</sub>)-hPmnCC; (iii) coinjection of product of partial digestion with pure dA-p(BH<sub>3</sub>)-hPmn II.

the PBH<sub>3</sub> diastereomer. The conventional method for making such stereochemical assignments for phosphorothioate- and boranophosphate-containing oligonucleotides is stereospecific enzymatic digestion with snake venom phosphodiesterase (SVP).<sup>27,28</sup> However, this enzyme only digests substrates containing a free 3'-hydroxyl group. These inhibitors contain an internal 3'-3' linkage and thus have two 5'-termini, but no 3' termini (Figure 1C). Therefore, they are not substrates for SVP. To circumvent this challenge, we synthesized the dinucleotide core of the PBH<sub>3</sub> inhibitor, dA-p(BH<sub>3</sub>)-hPmn, and used the two resulting diastereomers as standards for assigning the stereochemistry of the hexanucleotide (Figure 3A). We also prepared both diastereomers of the standard 5'-3' linked dinucleotide, dA-p(BH<sub>3</sub>)-A to assist with the stereochemical assignment. The diastereomers were purified by HPLC with baseline resolution as described in the Materials and Methods section.

Nuclease P1 does not require a 3'-terminus, and both the 5'-3' and the 3'-3' linked dinucleotides are substrates of this enzyme. However, the stereospecificity of the nuclease P1 for cleavage of boranophosphate linkages has not been established. Therefore, we first determined the diastereomeric preference of nuclease P1 using the 5'-3' dinucleotide dA-p(BH<sub>3</sub>)-A and obtained the absolute stereochemical assignment by comparison to the degradation of this substrate by SVP, the enzyme for which the stereochemical preference is known. With this information in hand, the preference of nuclease P1 for the 3'-3' linked inhibitor core was determined, which was used to assign the absolute stereochemistry of the two dA-p(BH<sub>3</sub>)-hPmn diastereomers. This was used to define the stereochemistry of the hexameric PBH<sub>3</sub> inhibitor by partial digestion to the dinucleotide core and RP-HPLC coinjection with the characterized dinucleotide standards.

SVP preferentially cleaves the S<sub>p</sub> diastereomer of the 5'-3' boranophosphate linkage as shown previously using the ribose dinucleotide, A-p(BH<sub>3</sub>)-A.<sup>28</sup> This is the diastereomer that contains the borano group in the oxyanion position. Consistent with these results, dA-p(BH<sub>3</sub>)-A I (HPLC-fast moving peak) was selectively cleaved by SVP (about 50% cleavage within 10 min), while dA-p(BH<sub>3</sub>)-A II was completely resistant over 220 min (Figure 3B). As a reference, the dApA phosphate control was completely degraded within the first minute. This suggests that dA-p(BH<sub>3</sub>)-A I is the S<sub>p</sub> diastereomer and contains the borano group in the oxyanion position. We repeated this analysis with nuclease P1 and found the opposite stereochemical preference. The dA-p(BH<sub>3</sub>)-A II was selectively cleaved (about 50% cleavage within 30 min), while dA-p(BH<sub>3</sub>)-A I was essentially resistant over 240 min (Figure 3C). As in the case of SVP, the reference dApA phosphate was about 100% cleaved within the first minute. This suggests that SVP and nuclease P1 have opposite stereochemical preference for the 5'-3' boranophosphate linkage (Figure 3B,C). Nuclease P1 cleaves the R<sub>p</sub> diastereomer, which has the oxygen rather than the borano group in the oxyanion position.

The next step in the stereochemical assignment was to use the diastereomeric preference of nuclease P1 to assign the isomers of the 3'-3' linked dinucleotide, dA-p(BH<sub>3</sub>)-hPmn (Figure 3A). On the basis of Prelog's priority rules,<sup>29</sup> the S<sub>p</sub> and R<sub>p</sub> designations are reversed relative to those in the 5'-3' linked dinucleotide, dA-p(BH<sub>3</sub>)-A. Thus, it is expected that nuclease P1 will selectively degrade the S<sub>p</sub> diastereomer, which has the oxygen in the oxyanion position, but the R<sub>p</sub> diastereomer with the borano group in the oxyanion position will be resistant. The two dA-p(BH<sub>3</sub>)-hPmn diastereomers were subjected to P1 nuclease digestion. dA-p(BH<sub>3</sub>)-hPmn I was selectively degraded by nuclease P1 (>90% cleavage within 30 min), while dA-p(BH<sub>3</sub>)-hPmn II was only about 10% cleaved over

120 min (Figure 3D). This indicates that dA-p(BH<sub>3</sub>)-hPmn II is the *R<sub>p</sub>* diastereomer and has the borano group in the oxyanion position. The reference phosphate dA-p-hPmn dinucleotide was quickly degraded by the enzyme.

To establish the stereochemical configuration of the hexanucleotide CCdA-p(BH<sub>3</sub>)-hPmnCC that was used in the ribosome binding studies, we partially digested CCdA-p(BH<sub>3</sub>)-hPmnCC with nuclease P1 (Figure 3E). The cytosines on each of the 5'-ends were quickly removed to produce the dinucleotide core, dA-p(BH<sub>3</sub>)-hPmn (see Figure 3A). The product of this partial digestion was analyzed on RP-HPLC against the reference dA-p(BH<sub>3</sub>)-hPmn for which the stereochemistry was determined (see above). Partial digestion produced a single dinucleotide peak that was resistant to nuclease P1 digestion even after more extensive digestion (Supporting Information Figure S7). This peak coeluted on RP-HPLC with the dA-p(BH<sub>3</sub>)-hPmn II dinucleotide inhibitor corresponding to the *R<sub>p</sub>* isomer in which the borano group mimics the oxyanion (Figure 3E).

The observation of a single HPLC peak resulting from the hexameric PBH<sub>3</sub> inhibitor synthesis was unexpected. One possible explanation was that both hexamers were produced in similar quantities, but they could not be resolved by the standard HPLC protocol. However, no expansion or alteration of the gradient produced any indication that there were two overlapping peaks. Furthermore, partial degradation by RNase A, which mechanistically requires a 2'-hydroxyl and thus cannot degrade the dinucleotide core, produced only one peak corresponding to dA-p(BH<sub>3</sub>)-hPmn II under conditions where we are certain both diastereomers could be resolved on HPLC (Supporting Information Figure S8). The absence of a second peak corresponding to dinucleotide dA-p(BH<sub>3</sub>)-hPmn I provides evidence that the hexamer was obtained as a pure *R<sub>p</sub>* diastereomer rather than a racemic mixture of both diastereomers. We also observed only one major peak for the synthesis of the dinucleotide inhibitor, dA-p(BH<sub>3</sub>)-hPmn II (Supporting Information Figure S4). The other diastereomer, dA-p(BH<sub>3</sub>)-hPmn I, also proved to be labile (see Supporting Information), but we were able to obtain a small amount of the dA-p(BH<sub>3</sub>)-hPmn I diastereomer to perform the stereochemical assignment. It is unclear why the *S<sub>p</sub>* diastereomer is preferentially degraded in the context of both the hexanucleotide and the dinucleotide inhibitors.

**Measuring Inhibitor Binding Affinities.** The relative magnitude of charge stabilization for each transition state mimic was estimated by measuring the equilibrium binding affinity (*K<sub>d</sub>*) of each inhibitor for the PTC. We determined the affinity using the well-established technique of RNA chemical modification.<sup>19</sup> The PTC residue A2602 in the 50S *E. coli* ribosome was probed using dimethyl sulfate as a function of inhibitor concentration. The PO inhibitor bound with an affinity of 160 nM (Table 1). This value represents the lower limit if charge stabilization is important and provides a benchmark for comparison.

The PMe diastereomeric inhibitors replace a negative charge in the PO inhibitor with a neutral methyl group (Figure 1C). Previous studies with nucleases that utilize electrostatic and hydrogen bond interactions have demonstrated that a methylphosphonate modification at the substrate cleavage site inactivates the enzyme.<sup>22</sup> We used a similar strategy to probe the electrostatic and hydrogen bond interactions of the ribosome with the oxyanion. Although the methyl group is uncharged, the remaining nonbridging oxygen retains a partial

**Table 1. Relative Binding Affinities of Peptidyl Transferase Inhibitors**

	PO	PCH <sub>3</sub> I <sup>a</sup>	PCH <sub>3</sub> II <sup>b</sup>	PBH <sub>3</sub>
<i>K<sub>d</sub></i> (nM) <sup>c</sup>	160 ± 30	170 ± 20	280 ± 60	460 ± 10
rel change <sup>d</sup>		1.1	1.8	2.9
ΔΔ <i>G</i> (kcal/mol)		0.04	0.3	0.6

<sup>a</sup>HPLC-fast eluting peak. <sup>b</sup>HPLC-slow eluting peak. <sup>c</sup>Each value is the average of at least three independent measurements. <sup>d</sup>Change in binding affinity is relative to the phosphate inhibitor.

negative charge.<sup>26</sup> Therefore, the effect of this substitution is to place a nearly isosteric, uncharged methyl group in place of one nonbridging oxygen. If the ribosome stabilizes the oxyanion, the PMe diastereomer whose methyl group mimics the oxyanion is expected to incur a significant loss in binding energy. The other PMe diastereomer, where the methyl group mimics the nascent peptide, is expected to exhibit similar binding energy to the PO inhibitor. We observed that the PMe I (HPLC fast-moving peak) bound with an affinity of 170 nM, which is essentially the same as that of the PO inhibitor. The other PMe inhibitor bound with an affinity of 280 nM. This binding corresponds to a loss in binding energy of only 0.3 kcal/mol relative to the PO control. Because the affinities of the two inhibitors were so similar, we did not make the effort to establish their absolute stereochemistry. Nevertheless, these results indicate that the maximal effect obtained by substituting a methyl group for an oxygen in the oxyanion position is less than 2-fold.

To further investigate this question, we synthesized a PBH<sub>3</sub> inhibitor CCdA-p(BH<sub>3</sub>)-hPmnCC that contains a borano group in the oxyanion position (Figure 1C). This PB inhibitor carries a formal negative charge but cannot form hydrogen-bonding interactions.<sup>24</sup> If the oxyanion is significantly stabilized by hydrogen bonding to the water molecule, this inhibitor should show a substantial loss in binding free energy. We found that the binding affinity of this inhibitor was 460 nM. Although the affinity is weaker, it is less than 3-fold different (0.6 kcal/mol) relative to the PO inhibitor and less than 2-fold relative to the weaker binding PMe inhibitor. Thus, we observed an effect on binding that was, at most, comparable in magnitude to that expected for a weak hydrogen bond.

## DISCUSSION

Many enzymes stabilize the oxyanion in the transition state as a strategy to accelerate the rate of reactions they catalyze.<sup>30,31</sup> Here we biochemically investigated the capacity of the ribosome to stabilize the oxyanion in the peptidyl transferase reaction using transition state inhibitors. The data indicate that the ribosome provides minimal transition state stabilization to the oxyanion. Substituting a neutral methyl group or a negatively charged, but non-hydrogen-bonding, borano group for the oxyanion had less than a 0.6 kcal/mol upon the binding free energy of the inhibitor. This level of stabilization is less than or equal to that expected for a weak hydrogen bond.

The magnitude of this effect can be better understood if put in context with studies performed on serine proteases. The contribution to stabilization of the transition state oxyanion by a single hydrogen bond has been calculated to be at least 3.7 kcal/mol using site-specific mutations.<sup>32,33</sup> In cutinase, an esterase, where the oxyanion is stabilized by two main-chain amide hydrogen bonds and a serine side chain, removal of the serine side chain hydrogen bond donor reduced the rate by

about 2000-fold.<sup>34</sup> Similarly, in subtilisin,<sup>35</sup> papain,<sup>36</sup> and lipase,<sup>37</sup> where the side chain also provides the hydrogen bond donor in the form of  $-NH$  or  $-OH$ , removal of these groups decreased the rate of the reaction by about 1000-fold.

But how comparable are rate effects in serine proteases to ribosomal binding effects using transition state inhibitors? Similar to what is proposed for peptide bond formation in the ribosome, the proteolytic reaction catalyzed by  $\alpha$ -chymotrypsin occurs via a tetrahedral-like transition state with a developing oxyanion. Inhibition studies using irreversible inhibitors containing a chiral methylphosphonate have been conducted on this enzyme to evaluate its enantioselectivity for either diastereomeric inhibitor. In contrast to the less than 2-fold binding effect that we observed when using the PT methylphosphonate inhibitors, the relative rates of inhibition of  $\alpha$ -chymotrypsin by the two diastereomers ranged from 90- to 1900-fold.<sup>38</sup> This finding highlights how placement of a neutral, methyl group at the oxyanion position can significantly impact the binding properties of an inhibitor for an enzyme that utilizes significant oxyanion stabilization.

The minimal stabilizing contribution of the ribosome for the oxyanion is also evident in the binding affinities of chiral phosphorothioate inhibitors. The sulfhydryl group is known to participate in hydrogen bonds, although its stabilizing contribution has only been estimated to be about 1 kcal/mol.<sup>39,40</sup> It is larger and more easily polarizable than oxygen<sup>41</sup> and, therefore, is a good mimic to investigate the developing negative charge in the transition state. The binding affinities for the PTC of phosphorothioate inhibitors containing the same general structures (CCA-p(S)-hPmnCC) as the inhibitors used in this study have been reported.<sup>5</sup> The two diastereomers bound with similar affinities (220 nM vs 250 nM). Similar studies also found that other phosphorothioate inhibitors that contained sulfur and methyl carboxylate groups as mimics of the oxyanion and the nascent peptide bound at 77 and 1500 nM, respectively.<sup>5</sup> Combined, these results demonstrate that the ribosome does not distinguish between a sulfur and an oxygen at the oxyanion position. However, a much larger group can exhibit a 20-fold effect in binding affinity, most likely due to steric hindrance. By contrast, the sulfur effect in TS stabilization of the oxyanion by serine proteases has previously been biochemically investigated. Substitution of sulfur for the carbonyl oxygen in the substrates for chymotrypsin and subtilisin completely abolished the reaction,<sup>42</sup> which illustrates the significance of TS stabilization of the oxyanion in enzymatic catalysis.

How effective is a water molecule bound to an enzyme active site in stabilizing a transition state oxyanion? Water molecules undoubtedly stabilize the oxyanion of the uncatalyzed reaction in solution. Additional catalysis may be provided if the water is bound to the enzyme at a lower entropic cost than the ordering of water molecules around the transition state in solution.<sup>43</sup> Conversely, the enzyme-bound water molecule may be no more favorable than the water found in solution but simply avoids an energy penalty associated with removing the oxyanion from any source of stabilization. Though rare, water molecules have been observed in enzyme oxyanion holes, most commonly in the thiolase superfamily enzymes. In the thiolase-catalyzed Claisen condensation reaction between acetyl-CoA and the acetylated form of the enzyme, the oxyanion of the enolate intermediate forms hydrogen bonds with both a His residue and a water molecule.<sup>44</sup> This water is anchored in the active site via hydrogen-bonding interactions to a highly

conserved Asn residue. Mutation of the Asn residue impairs the reaction, which suggests that the water molecule is important for stabilizing the oxyanion.

On the basis of structural and molecular dynamic studies, the water molecule within the ribosome adopts a geometry that positions it as the only possible stabilizing partner of the oxyanion.<sup>9</sup> Recent studies indicate the geometry of the active site is a significant factor in stabilizing an oxyanion.<sup>45</sup> The active site of ketosteroid isomerase is rigid enough to preferentially match the distance from hydrogen bond donors to the transition-state oxyanion versus the ground-state carbonyl. In the ribosome, the water molecule is anchored in the active site via residues A2602 and U2584 and appears to be highly ordered and completely desolvated (Figure 2). It is expected that any mutation that affects the geometry of this water in the ribosome would also affect the rate of the peptidyl transferase reaction if transition state stabilization of the oxyanion is important. Yet, mutation of residue A2602 to G, U, or C had only minimal effects (less than 2-fold) on the rate of peptide bond formation.<sup>46</sup> This observation, which was obtained using a completely different approach, is in agreement with the data presented in the current study and suggests that the ribosome provides only minimal energy to stabilize the oxyanion in the transition state.

We cannot exclude the possibility that these phosphorus-based PT inhibitors do not mimic the transition state of peptide bond formation with sufficient accuracy to address the role of oxyanion stabilization in the reaction. The actual transition state is not fully tetrahedral, and the bond lengths, bond angles, and local charges are all fractionally different than the phosphate mimic that serves as the basis for affinity comparison of the various derivatives. However, studies using similar analogues in other systems where oxyanion stabilization does play a significant role found much larger effects on inhibitor binding affinities than were observed here.<sup>37</sup> Furthermore, large effects on hexameric inhibitor affinities were observed in this system for studies that explored the regio- and stereospecificity of the PT reaction.<sup>5</sup>

The analogue binding and mutational data suggest that the PT reaction proceeds through a transition state that does not require stabilization of the negative charge on the carbonyl oxygen by functional groups in an oxyanion hole. One possible rationalization of these data is that the reaction does not proceed through a tetrahedral-like intermediate because the reaction is fully concerted with simultaneous C–N bond formation and C–O3' bond breaking. In this scenario the tetrahedral phosphate-based inhibitors would be particularly poor mimics of the transition state because the carbonyl carbon retains its  $sp^2$  bonding character and bonding to the carbonyl oxygen is largely unaffected. However, recent data are not consistent with this fully concerted model for peptide bond formation.<sup>11</sup>

The nature of the transition state was recently addressed using KIE analysis, which demonstrated that the reaction is not concerted.<sup>11</sup> The data support a two-step reaction mechanism in which C–N bond formation is rate-limiting and the C–O3' bond remains intact in the transition state. Although the transition state is early, with a C–N bond distance of  $\sim 1.8$  Å, there is significant tetrahedral geometry. This is expected to correspond to a partially charged oxyanion. Brønsted analysis of the  $\alpha$ -amino group suggests that C–N bond formation occurs with commensurate deprotonation of the  $\alpha$ -amine because there is no change in charge on the amine between the ground



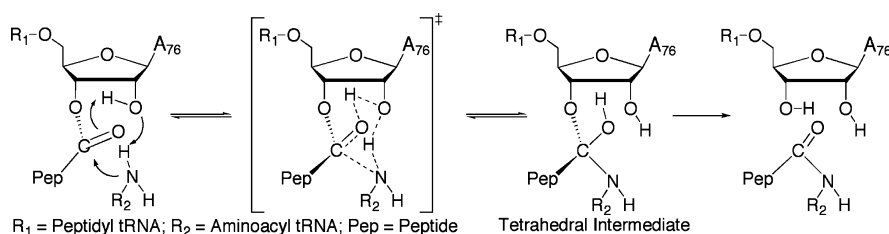


**Figure 4.** Possible stabilization of the oxanion via a stepwise, proton shuttle mechanism. In this model, C–N bond formation is commensurate with deprotonation of the  $\alpha$ -amino group by the 2'-OH, which in turn donates its proton to the carbonyl carbon. This leads to a neutral tetrahedral intermediate that collapses into product after C–O3' bond breaking accompanied by proton transfer from the carbonyl oxygen to either the O3'-leaving group or the 2'-OH mediated via a water molecule.<sup>12</sup>

state and the transition state.<sup>47</sup> Deuterium solvent isotope effect analysis provided a proton inventory to establish that there were multiple protons in flight in the transition state.<sup>12</sup> One of these is likely to be the  $\alpha$ -amino proton. A second could be the A76 2'-OH, which in turn might be shuttled to a second ordered water molecule within the active site. As an alternative or in addition to the water molecule, the proton could be shuttled to the oxanion as has been suggested based on computational studies.<sup>48,49</sup> This mechanism couples deprotonation of the amine and protonation of the oxanion, resulting in a neutral tetrahedral-like transition state (Figure 4). In this scenario, instead of activating the O3' leaving group in a concerted reaction mechanism, as originally proposed, the proton shuttle would provide charge stabilization for the oxanion. This would minimize the need for oxanion stabilization by the water molecule or other ribosomal groups within the PTC. Such a mechanism was recently proposed based upon the number of protons in flight in the transition state.<sup>12</sup>

In summary, these data suggest that the ribosome provides minimal transition state stabilization to the oxanion via a water molecule. Although the role of this water molecule seems to be minimal in the peptidyl transferase reaction, mutational data suggest that it might play a more prominent catalytic role in peptide release.<sup>46</sup> If so, this catalytic dichotomy might provide clues as to how the ribosome may have evolved to accommodate and fine-tune two biologically essential but competing reactions within the same active site.

## ■ ASSOCIATED CONTENT

### ● Supporting Information

Evidence supporting the chemical degradation of one of the CCdA-p(BH<sub>3</sub>)-hPmnCC diastereomers. This material is available free of charge via the Internet at <http://pubs.acs.org>.

## ■ AUTHOR INFORMATION

### Corresponding Author

\*Phone: 203-432-9772. Fax: 203-432-5767. E-mail: [scott.strobel@yale.edu](mailto:scott.strobel@yale.edu).

### Present Address

<sup>†</sup>Department of Chemistry & Physical Science, Quinnipiac University, 275 Mount Carmel Ave., Hamden, CT 06518-1908.

### Funding

This work was supported by NIH grant GM54839 to S.A.S. and NIH Postdoctoral Fellowship F32 GM 076918 to N.C.

## ■ ACKNOWLEDGMENTS

We thank Vipender Singh for performing computational calculations on some of the inhibitors.

## ■ ABBREVIATIONS

PTC, peptidyl transferase center; Pmn, puromycin; hPmn, hydroxypuromycin; PT, peptidyl transferase; DMTr, dimethoxytrityl; TEAAc, triethylammonium acetate; TS, transition state.

## ■ REFERENCES

- (1) Schmeing, T. M., and Ramakrishnan, V. (2009) What recent ribosome structures have revealed about the mechanism of translation. *Nature* 461, 1234–1242.
- (2) Nissen, P., Hansen, J., Ban, N., Moore, P. B., and Steitz, T. A. (2000) The structural basis of ribosome activity in peptide bond synthesis. *Science* 289, 920–930.
- (3) Weinger, J. S., Parnell, K. M., Dörner, S., Green, R., and Strobel, S. A. (2004) Substrate-assisted catalysis of peptide bond formation by the ribosome. *Nat. Struct. Mol. Biol.* 11, 1101–1106.
- (4) Zaher, H. S., Shaw, J. J., Strobel, S. A., and Green, R. (2011) The 2'-OH group of the peptidyl-tRNA stabilizes an active conformation of the ribosomal PTC. *EMBO J.* 30, 2445–2453.
- (5) Huang, K. S., Carrasco, N., Pfund, E., and Strobel, S. A. (2008) Transition state chirality and role of the vicinal hydroxyl in the ribosomal peptidyl transferase reaction. *Biochemistry* 47, 8822–8827.
- (6) Erlacher, M. D., Lang, K., Wotzel, B., Rieder, R., Micura, R., and Polacek, N. (2006) Efficient ribosomal peptidyl transfer critically relies on the presence of the ribose 2'-OH at A2451 of 23S rRNA. *J. Am. Chem. Soc.* 128, 4453–4459.
- (7) Trobro, S., and Aqvist, J. (2005) Mechanism of peptide bond synthesis on the ribosome. *Proc. Natl. Acad. Sci. U. S. A.* 102, 12395–12400.
- (8) Trobro, S., and Aqvist, J. (2006) Analysis of predictions for the catalytic mechanism of ribosomal peptidyl transfer. *Biochemistry* 45, 7049–7056.
- (9) Schmeing, T. M., Huang, K. S., Kitchen, D. E., Strobel, S. A., and Steitz, T. A. (2005) Structural insights into the roles of water and the 2' hydroxyl of the P site tRNA in the peptidyl transferase reaction. *Mol. Cell* 20, 437–448.
- (10) Dörner, S., Panuschka, C., Schmid, W., and Barta, A. (2003) Mononucleotide derivatives as ribosomal P-site substrates reveal an important contribution of the 2'-OH to activity. *Nucleic Acids Res.* 31, 6536–6542.
- (11) Hiller, D. A., Singh, V., and Strobel, S. A. (2011) A Two-step Chemical Mechanism for Ribosome-Catalyzed Peptide Bond Formation. *Nature* 476, 236–239.
- (12) Kuhlencoetter, S., Wintermeyer, W., and Rodnina, M. V. (2011) Different substrate-dependent transition states in the active site of the ribosome. *Nature* 476, 351–354.
- (13) Wallin, G., and Aqvist, J. (2010) The transition state for peptide bond formation reveals the ribosome as a water trap. *Proc. Natl. Acad. Sci. U. S. A.* 107, 1888–1893.
- (14) Weinger, J. S., Kitchen, D., Scaringe, S. A., Strobel, S. A., and Muth, G. W. (2004) Solid phase synthesis and binding affinity of peptidyl transferase transition state mimics containing 2'-OH at P-site position A76. *Nucleic Acids Res.* 32, 1502–1511.

- (15) Li, P., Sergueeva, Z. A., Dobrikov, M., and Shaw, B. R. (2007) Nucleoside and oligonucleoside boranophosphates: chemistry and properties. *Chem. Rev.* 107, 4746–4796.
- (16) Hyodo, M., and Hayakawa, Y. (2006) Nucleobase Protection with Allyloxycarbonyl, in *Current Protocols in Nucleic Acid Chemistry* (Beaucage, S. L., Bergstrom, D. E., Herdewijn, P., and Matsuda, A., Eds.) John Wiley & Sons, Inc., Hoboken, NJ.
- (17) McCuen, H. B., Noe, M. S., Sierzchala, A. B., Higson, A. P., and Caruthers, M. H. (2006) Synthesis of mixed sequence borane phosphonate DNA. *J. Am. Chem. Soc.* 128, 8138–8139.
- (18) Hayakawa, Y., Hirose, M., and Noyori, R. (1993) O-Allyl protection of guanine and thymine residues in oligodeoxyribonucleotides. *J. Org. Chem.* 58, 5551–5555.
- (19) Parnell, K. M., Seila, A. C., and Strobel, S. A. (2002) Evidence against stabilization of the transition state oxyanion by a pKa-perturbed RNA base in the peptidyl transferase center. *Proc. Natl. Acad. Sci. U. S. A.* 99, 11658–11663.
- (20) Welch, M., Chastang, J., and Yarus, M. (1995) An inhibitor of ribosomal peptidyl transferase using transition-state analogy. *Biochemistry* 34, 385–903.
- (21) Schmeing, T. M., Huang, K. S., Strobel, S. A., and Steitz, T. A. (2005) An induced-fit mechanism to promote peptide bond formation and exclude hydrolysis of peptidyl-tRNA. *Nature* 438, 520–524.
- (22) Srivastava, T. K., Friedhoff, P., Pingoud, A., and Katti, S. B. (1999) Application of oligonucleoside methylphosphonates in the studies on phosphodiester hydrolysis by Serratia endonuclease. *Nucleosides Nucleotides* 18, 1945–1960.
- (23) Dertinger, D., and Uhlenbeck, O. C. (2001) Evaluation of methylphosphonates as analogs for detecting phosphate contacts in RNA-protein complexes. *RNA* 7, 622–631.
- (24) Nahum, V., and Fischer, B. (2004) Boranophosphate Salts as an Excellent Mimic of Phosphate Salts: Preparation, Characterization, and Properties. *Eur. J. Inorg. Chem.*, 4124–4131.
- (25) Schramm, V. L. (2011) Enzymatic transition States, transition-state analogs, dynamics, thermodynamics, and lifetimes. *Annu. Rev. Biochem.* 80, 703–732.
- (26) Stivers, J. T., and Nagarajan, R. (2006) Probing Enzyme Phosphodiester Interactions by Combining Mutagenesis and Chemical Modification of Phosphate Ester Oxygens. *Chem. Rev.* 106, 3443–3467.
- (27) Burgers, P. M., Eckstein, F., and Hunneman, D. H. (1979) Stereochemistry of hydrolysis by snake venom phosphodiesterase. *J. Biol. Chem.* 254, 7476–7478.
- (28) Enya, Y., Nagata, S., Masutomi, Y., Kitagawa, H., Takagaki, K., Oka, N., Wada, T., Ohgi, T., and Yano, J. (2008) Chemical synthesis of diastereomeric diadenosine boranophosphates (A<sub>p</sub>B<sub>A</sub>) from 2'-O-(2-cyanoethoxymethyl)adenosine by the boranophosphotriester method. *Bioorg. Med. Chem.* 16, 9154–9160.
- (29) Cahn, R. S., Ingold, C., and Prelog, V. (1966) Specification of Molecular Chirality. *Angew. Chem., Int. Ed. Engl.* 5, 385–415.
- (30) Kraut, J. (1977) Serine proteases: structure and mechanism of catalysis. *Annu. Rev. Biochem.* 46, 331–358.
- (31) Menard, R., and Storer, A. C. (1992) Oxyanion hole interactions in serine and cysteine proteases. *Biol. Chem. Hoppe Seyler* 373, 393–400.
- (32) Fersht, A. R. (1999) *Structure and Mechanism in Protein Science*, pp 472–490, W.H. Freeman and Company, New York.
- (33) Fersht, A. R., Shi, J. P., Knill-Jones, J., Lowe, D. M., Wilkinson, A. J., Blow, D. M., Brick, P., Carter, P., Waye, M. M., and Winter, G. (1985) Hydrogen bonding and biological specificity analysed by protein engineering. *Nature* 314, 235–238.
- (34) Nicolas, A., Egmond, M., Verrips, C. T., de Vlieg, J., Longhi, S., Cambillau, C., and Martinez, C. (1996) Contribution of cutinase serine 42 side chain to the stabilization of the oxyanion transition state. *Biochemistry* 35, 398–410.
- (35) Wells, J. A., Cunningham, B. C., Graycar, T. P., and Estell, D. A. (1986) Importance of Hydrogen-Bond Formation in Stabilizing the Transition State of Subtilisin. *Philos. Trans. R. Soc., A* 317, 415–423.
- (36) Menard, R., Carriere, J., Laflamme, P., Plouffe, C., Khouri, H. E., Vernet, T., Tessier, D. C., Thomas, D. Y., and Storer, A. C. (1991) Contribution of the glutamine 19 side chain to transition-state stabilization in the oxyanion hole of papain. *Biochemistry* 30, 8924–8928.
- (37) Magnusson, A., Hult, K., and Holmquist, M. (2001) Creation of an enantioselective hydrolase by engineered substrate-assisted catalysis. *J. Am. Chem. Soc.* 123, 4354–4355.
- (38) Zhao, Q., Kovach, I. M., Bencsura, A., and Papathanassiou, A. (1994) Enantioselective and reversible inhibition of trypsin and alpha-chymotrypsin by phosphonate esters. *Biochemistry* 33, 8128–8138.
- (39) Wilkinson, A. J., Fersht, A. R., Blow, D. M., and Winter, G. (1983) Site-directed mutagenesis as a probe of enzyme structure and catalysis: tyrosyl-tRNA synthetase cysteine-35 to glycine-35 mutation. *Biochemistry* 22, 3581–3586.
- (40) Sabin, J. R. (1971) Hydrogen Bonds Involving Sulfur. I. The Hydrogen Sulfide Dimer. *J. Am. Chem. Soc.* 93, 3613–3620.
- (41) Horton, D. (2002) *Advances in Carbohydrate Chemistry and Biochemistry*, p 22, Academic Press, New York.
- (42) Asboth, B., and Polgar, L. (1983) Transition-state stabilization at the oxyanion binding sites of serine and thiol proteinases: hydrolyses of thiono and oxygen esters. *Biochemistry* 22, 117–122.
- (43) Jencks, W. P. (1975) Binding energy, specificity and enzymic catalysis: The Circe effect. *Adv. Enzymol. Relat. Areas Mol. Biol.* 43, 219–410.
- (44) Merilainen, G., Poikela, V., Kursula, P., and Wierenga, R. K. (2009) The thiolase reaction mechanism: the importance of Asn316 and His348 for stabilizing the enolate intermediate of the Claisen condensation. *Biochemistry* 48, 11011–11025.
- (45) Sigala, P. A., Kraut, D. A., Caaveiro, J. M. M., Pybus, B., Ruben, E. A., Ringe, D., Petsko, G. A., and Herschlag, D. (2008) Testing geometrical discrimination within an enzyme active site: constrained hydrogen bonding in the ketosteroid isomerase oxyanion hole. *J. Am. Chem. Soc.* 130, 13696–13708.
- (46) Youngman, E. M., Brunelle, J. L., Kochaniak, A. B., and Green, R. (2004) The active site of the ribosome is composed of two layers of conserved nucleotides with distinct roles in peptide bond formation and peptide release. *Cell* 117, 589–599.
- (47) Kingery, D. A., Pfund, E., Voorhees, R. M., Okuda, K., Wohlgemuth, I., Kitchen, D. E., Rodnina, M. V., and Strobel, S. A. (2008) An uncharged amine in the transition state of the ribosomal peptidyl transfer reaction. *Chem. Biol.* 15, 493–500.
- (48) Wang, Q., Gao, J., Liu, Y., and Liu, C. (2010) Validating a new proton shuttle reaction pathway for formation of the peptide bond in ribosomes: A theoretical investigation. *Chem. Phys. Lett.* 501, 113–117.
- (49) Rangelov, M. A., Petrova, G. P., Yomtova, V. M., and Vayssilov, G. N. (2010) Catalytic Role of Vicinal OH in Ester Aminolysis: Proton Shuttle versus Hydrogen Bond Stabilization. *J. Org. Chem.* 75, 6782–6792.